Available online at www.sciencedirect.com
ScienceDirect
Trans. Nonferrous Met. Soc. China 28(2018) 2011−2016
Transactions of Nonferrous Metals Society of China
www.tnmsc.cn

In situ formation of $Zr_2Al_3C_4/Al_2O_3$ composites by combustion synthesis with PTFE and thermal activations

Chun-Liang YEH, Yi-Chang CHEN

Department of Aerospace and Systems Engineering,
Feng Chia University, 100 Wenhwa Road, Seatwen, Taichung 40724, Taiwan, China

Received 20 December 2017; accepted 8 March 2018

Abstract: Preparation of $Zr_2Al_3C_4$−Al_2O_3 in situ composites was investigated by self-propagating high-temperature synthesis (SHS) involving both aluminothermic reduction of ZrO_2 and chemical activation of PTFE (Teflon). The starting materials included ZrO_2, Al, carbon black and PTFE. In addition to the conventional SHS method, the experiments were conducted by a chemical-oven SHS (COSHS) route to thermally assist the synthesis reaction. The threshold amount of 2% (mass fraction) PTFE was required to induce self-sustaining combustion. When the conventional SHS scheme was utilized, due to low combustion temperatures between 1152 and 1272 °C and insufficient reaction time, the dominant carbide forming in the composite was ZrC instead of $Zr_2Al_3C_4$. On the other hand, the COSHS technique increased the combustion temperature of the reactant compact to about 1576 °C, lengthened the high-temperature duration for the reaction, and prevented Al vapor from escaping away. As a consequence, $Zr_2Al_3C_4$−Al_2O_3 composites with a small amount of $Zr_3Al_3C_5$ were obtained. The microstructure of the COSHS-derived product showed that plate-like $Zr_2Al_3C_4$ grains were about 2 μm in thickness and 10−30 μm in length, and most of them were closely stacked into a laminated configuration.

Key words: $Zr_2Al_3C_4$; combustion synthesis; PTFE activation; chemical-oven SHS; aluminothermic reduction

1 Introduction

Ternary aluminum carbides, such as Ti_2AlC and Ti_3AlC_2, known as the MAX phase, have low density, high stiffness, high thermal conductivity, and good oxidation and corrosion resistance at high temperatures, as ceramics; while they are relatively soft, readily machinable, electrically conductive, resistant to thermal shock, and highly tolerable to damage, as metals [1−3]. In the Zr−Al−C ternary system, $Zr_2Al_3C_4$ has a hexagonal crystal structure [4] and possesses much better oxidation resistance than ZrC and comparable high-temperature mechanical properties to ultra-high temperature ceramics (UHTCs), such as ZrB_2−SiC and HfB_2−SiC composites [5]. As a conductive ceramic, $Zr_2Al_3C_4$ is a promising reinforcement for Cu without any detrimental effect on the electrical conductivity [6].

$Zr_2Al_3C_4$ was first synthesized by SCHUSTER and NOWOTNY [7] via arc melting of a mixture of Zr or ZrC, Al, and C powders at 1000 °C. Afterwards, FUKADA et al [8] produced $Zr_2Al_3C_4$ together with small amounts of Al_2O_3 and $Zr_3Al_3C_5$ by heating a compressed pellet made up of ZrC, Al, and graphite at 1380 °C for 1 h in Ar. HE et al [9] fabricated bulk $Zr_2Al_3C_4$ from Zr, Al, and graphite powders by in situ reactive hot pressing at 1900 °C under 30 MPa for 1 h in Ar and then annealing at 1600 °C for 0.5 h in low vacuum. Preparation of $Zr_2Al_3C_4$ thin films was recently conducted by pulsed cathodic arc deposition from elemental Zr, Al and carbon cathodes [10]. With the use of Zr, Al, graphite and B_4C as the starting materials, $Zr_2Al_3C_4$−ZrB_2 composites were produced by spark plasma sintering [11]. The addition of ZrB_2 was shown to improve hardness, elastic modulus, fracture toughness, thermal conductivity, and oxidation resistance of $Zr_2Al_3C_4$ [11].

As a promising alternative, combustion synthesis in the mode of self-propagating high-temperature synthesis (SHS) takes advantage of the self-sustaining merit from the highly exothermic reaction, and hence, has the benefits of low energy requirement, short reaction time, high-purity products, and simple facilities [12,13]. The SHS technique has been applied to preparing the MAX

Corresponding author: Chun-liang YEH; Tel: +886-4-24517250; E-mail: clyeh@fcu.edu.tw
DOI: 10.1016/S1003-6326(18)64845-9

carbides, Ti_3AlC_2, Ti_2AlC and Ta_2AlC, from elemental powder compacts [14−16]. For the improvement in fracture toughness, flexural strength and hardness of ternary aluminum carbides, Al_2O_3 has been demonstrated as one of the effective reinforcing phases [17−19]. Previous studies showed that the SHS method involving aluminothermic reduction of metal oxides represented an in situ processing route capable of producing Al_2O_3-reinforced Ti_3AlC_2, Ti_2AlC, Nb_2AlC and NiAl [20−22]. Due mainly to weak exothermicity of reduction of ZrO_2 by Al, however, the $Zr_2Al_3C_4$−Al_2O_3 composite has not been investigated by the SHS process.

This work made the first attempt to prepare the $Zr_2Al_3C_4$−Al_2O_3 composite by combustion synthesis with a reduction stage. In order to chemically promote the SHS reaction, we adopt PTFE (polytetrafluoroethylene or Teflon) as an activator and carburizing agent. Besides, thermal activation is conducted by employing a modification of the conventional SHS method called chemical-oven SHS (COSHS), which provides extra heat flux to the sample and prolongs the high-temperature duration for the reaction [23,24]. In particular, the effects of chemical activation by PTFE and thermal boost by COSHS were investigated on combustion sustainability, combustion wave velocity, reaction temperature and product composition.

2 Experimental

The starting materials adopted in this work included ZrO_2 (Alfa Aesar Co., <45 μm, 99%), Al (Showa Chemical Co., <45 μm, 99.9%), carbon black (Showa Chemical Co., 20−40 nm, 99%), and PTFE (—$(C_2F_4)_n$—, Alfa Aesar Co., 6−10 μm). The mixture of reactant powders was formulated based upon the stoichiometry of Reaction (1):

$$6ZrO_2+17Al+(12-x)C+xC_{PTFE} \xrightarrow{-(C_2F_4)_n-} 3Zr_2Al_3C_4+4Al_2O_3 \quad (1)$$

where C_{PTFE} represents carbon supplied from complete decomposition of PTFE and is taken into account as a part in the total carbon balance. Reactant powders were well mixed and compressed into cylindrical samples with 7 mm in diameter, 12 mm in length, and a relative density of 55% for the test in the conventional SHS configuration. It was found that combustion ceased to propagate and quenched after ignition when no PTFE was added. The threshold amount of PTFE required for inducing self-sustaining combustion in Reaction (1) was experimentally determined to be 2% (mass fraction), which is correspondingly equivalent to x=0.54. As a reaction promoter, PTFE is able to peel off the Al_2O_3 shell on the surface of the Al particle and enhances the reactivity of Al powders [25]. As a carburizing agent, thermal decomposition of PTFE generates carbon (C_{PTFE}) that participates directly in the reaction [26,27]. The reactant compacts with 2%, 3%, and 4% (mass fraction) PTFE (i.e., x=0.54, 0.81, and 1.07) were conducted under the conventional SHS mode.

In the COSHS technique, composite test specimens were prepared that included a core reactant compact (7 mm in diameter and 10 mm in length) made up of the main mixture of Reaction (1) with 4% (mass fraction) PTFE and a shell composed of an equimolar Ti/C booster mixture. The resulting composite sample, as illustrated in Fig. 1, had a diameter of 12 mm and a height of 15 mm. Both SHS and COSHS experiments were performed in a windowed stainless-steel chamber under high purity argon (99.99%) of 0.15 MPa. A schematic diagram of the detailed experimental setup was presented elsewhere [28]. Ignition of either regular or composite samples was accomplished by a heated tungsten coil with a voltage of 60 V and a current of 1.5 A. The combustion process was recorded by a CCD video camera (Pulnix TMC−7). The combustion wave velocity was determined from the time sequence of recorded images. The combustion temperature was measured by a fine-wire (125 μm) Pt/Pt−13%Rh thermocouple attached on the sample surface. Phase constituents of the final product were identified by an X-ray diffractometer (Bruker D2) with Cu K_α radiation. The product microstructure was examined under a scanning electron microscope (Hitachi S3000N).

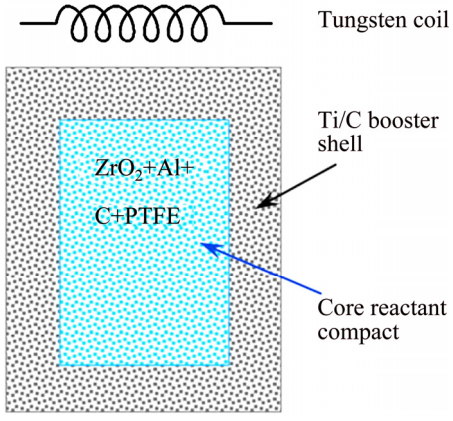

Fig. 1 Schematic diagram of composite sample for COSHS test

3 Results and discussion

3.1 Self-propagating combustion characteristics

Figure 2 presents a combustion sequence recorded from a 2% (mass fraction) PTFE-added powder compact ignited under the conventional SHS mode. As illustrated in Fig. 2, shortly after initiation, a localized reaction zone formed at the combustion front traveling along a spiral

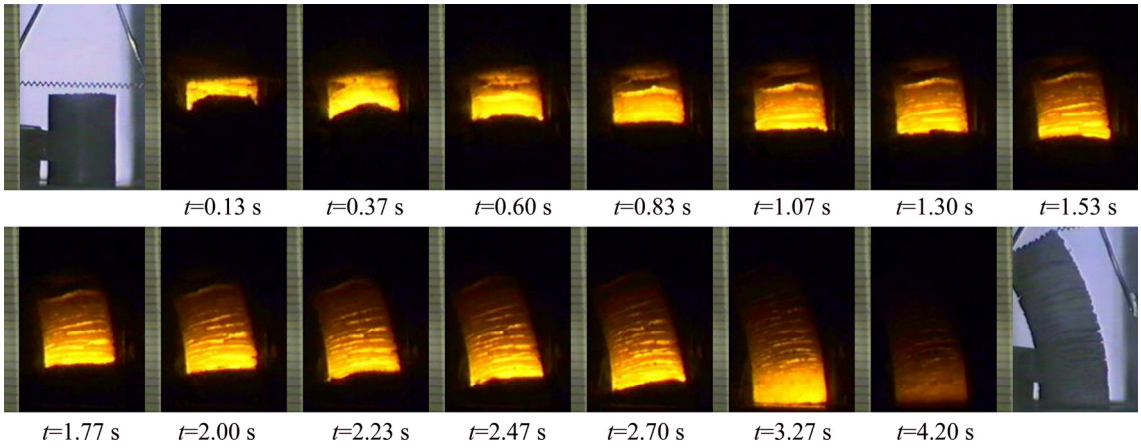

Fig. 2 Time sequence of self-propagating combustion images recorded from powder compact of Reaction (1) with addition of 2% PTFE

trajectory over the sample surface. It took about t=3.27 s for the combustion wave to propagate from the ignition plane to the bottom of the sample. The combustion front velocity (V_f) of about 3.18 mm/s was deduced from the time-sequence images. Moreover, the spinning combustion wave left visible corkscrew marks on the sample surface. The increase of PTFE increased the combustion velocity to V_f=3.68 mm/s at 3% PTFE and 4.31 mm/s at 4% PTFE, but did not change the combustion behavior. Figure 2 also reveals that the burned sample was subjected to axial elongation. This could be caused by the ejection of gaseous species from the powder compact, which cracked the burned sample. Consequently, due to fracture formation over the sample, the height of the sample was significantly increased. To be discussed below, gaseous species possibly formed from Reaction (1) are CO, F_2, and Al vapor. For the COSHS experiment, a burst of incandescent burning glow emitted almost volumetrically from the composite sample was detected. This suggests a highly energetic and fast combustion reaction occurring in the booster shell.

Propagation of self-sustaining combustion in a spinning manner is considered as an unstable SHS process. There are thermodynamic and kinetic reasons which provide the basis for departure from the steady condition [29]. Thermodynamic considerations arise from the degree of reaction exothermicity. Once the heat flux released from combustion is not enough to maintain longitudinal propagation of a planar reaction front, the combustion zone is confined to one or several reaction spots moving along a spiral path. Kinetic reasons are largely attributed to insufficient reactivity on account of the presence of diffusion barriers.

In Reaction (1), aluminothermic reduction of ZrO_2 with H_r=−24.8 kJ/mol of Al_2O_3 is weakly exothermic [30]. It is believed that for the PTFE-added sample, fluorine (F_2) generated from thermal decomposition of PTFE reacts with the reduced Zr and produces ZrF_4 along with a large formation enthalpy of H_f=−1911.3 kJ/mol [30], which has a great benefit to the SHS process. The highly reactive ZrF_4 subsequently reacts with carbon to yield ZrC and F_2. ZrC is an important intermediate for the evolution of $Zr_2Al_3C_4$ [9]. Moreover, the active interaction between PTFE and Al_2O_3 produces AlF_3 and CO, which removes the oxide shell on the Al particle surface [25]. As a result, the reactivity of Al and the degree of reduction of ZrO_2 were enhanced. The above PTFE-involving reactions confirm the role played by PTFE in the chemical activation.

3.2 Combustion temperatures of SHS and COSHS reactions

Combustion temperature profiles depicted in Fig. 3 were associated with PTFE-activated powder compacts conducted by the conventional SHS scheme. The rise in temperature signifies arrival of the combustion wave and the peak value corresponds to the combustion front temperature. After the passage of the combustion front, an appreciable decrease in temperature is a result of heat loss to the surroundings. The maximum temperature arrived at 1152 °C for the sample with addition of 2% PTFE and was further up to 1272 °C for the 4% PTFE-added sample. The increase of combustion front temperature with PTFE was attributed to a larger amount of ZrF_4 formed in the course of combustion synthesis. According to MUSA et al [27], the reaction exothermicity is enhanced by PTFE through formation of metal fluorides as intermediate phases. As mentioned above, fluorine (F_2) generated from PTFE reacts with the reduced Zr to produce ZrF_4 and a large reaction enthalpy [30]. However, the dwell time at the temperatures close to its peak value for the sample compact was very short and approximately 0.2−0.4 s.

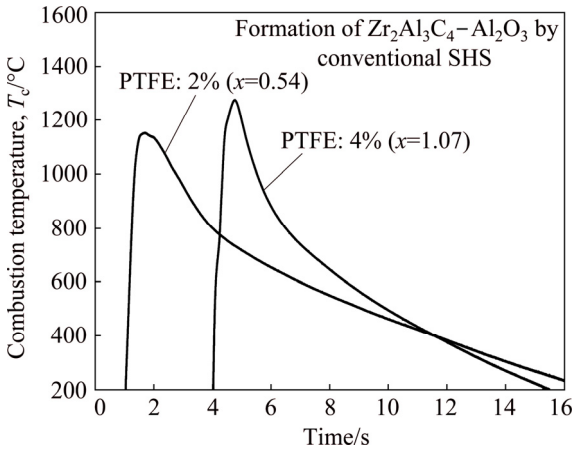

Fig. 3 Combustion temperature profiles of PTFE-activated samples under conventional SHS mode

Figure 4 shows the combustion temperature profiles measured from the booster shell and core reactant compact of a COSHS composite sample. For the Ti/C booster mixture, a nearly vertical temperature gradient signified an extremely fast reaction rate and the peak temperature reached as high as 1722 °C. The temperature curve of the core reactant compact exhibited an increase to a peak value of 1576 °C followed by a decrease to a plateau region, where the sample temperature was retained at about 1455 °C for 2.0−2.5 s. After that, the sample temperature decreased at a slower rate compared to that experienced by the sample in the conventional SHS process. It is evident that with the aid of COSHS the synthesis reaction was thermally boosted.

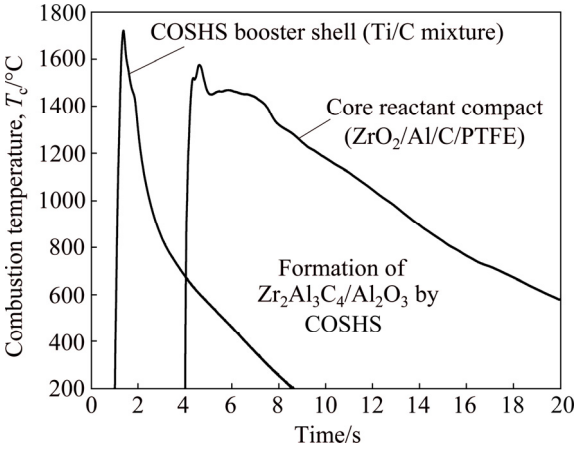

Fig. 4 Combustion temperature profiles of booster shell and core reactant compact of composite sample under COSHS mode

3.3 Phase constituents and microstructures of synthesized composites

Figures 5(a) and (b) display the XRD patterns of final products obtained from PTFE-added powder compacts conducted in a conventional SHS process. Figure 5(a) indicates that for the 2% PTFE-added sample, the resulting composite consisted of ZrC and Al_2O_3 as the major constituents. The Zr−Al−C ternary phase $Zr_2Al_3C_4$ was poorly formed and some ZrO_2 was found as the remnant. This suggested that not only the phase transformation from ZrC to $Zr_2Al_3C_4$ was incomplete, but also aluminothermic reduction of ZrO_2 was unfinished. Formation of $Zr_2Al_3C_4$ is considered to involve the reaction of ZrC, Al, and C. It is believed that weak exothermicity of the reaction (T_c=1152 °C) and evaporation loss of Al during the SHS process are responsible for the poor formation of $Zr_2Al_3C_4$.

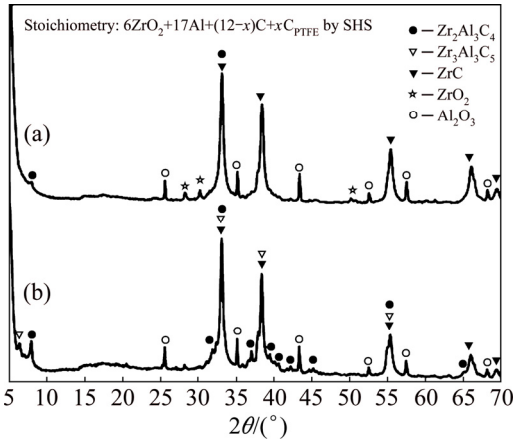

Fig. 5 XRD patterns of final products synthesized by conventional SHS from Reaction (1): (a) PTFE: 2% (x=0.54); (b) PTFE: 4% (x=1.07)

Figure 5(b) shows that for the sample containing 4% PTFE, the yield of $Zr_2Al_3C_4$ was slightly improved and the signature of ZrO_2 disappeared. This could be attributed to a higher combustion temperature of about 1272 °C. Other ternary carbide $Zr_3Al_3C_5$ was found in Fig. 5(b). According to HE et al [9], $Zr_3Al_3C_5$ was produced at high temperatures through the interaction of $Zr_2Al_3C_4$ with ZrC. Even though the formation of $Zr_2Al_3C_4$ was improved by increasing PTFE, ZrC was still the dominant carbide in the end product. This implied that evaporation loss of Al from the fissure-filled sample remained.

When the COSHS method was utilized, as revealed in Fig. 6, a $Zr_2Al_3C_4$−Al_2O_3 composite with a small amount of $Zr_3Al_3C_5$ was the end product. Compared with the conventional SHS process, the COSHS scheme substantially increased the reaction temperature (T_c=1576 °C) and prolonged the reaction time. Moreover, the booster shell could prevent Al vapor from escaping away. Therefore, phase evolution was practically completed.

The typical microstructures of fracture surface of the final products synthesized by the conventional SHS and COSHS processes are shown in Figs. 7(a) and (b),

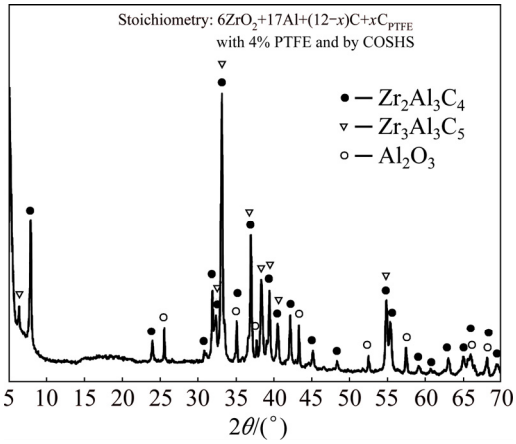

Fig. 6 XRD pattern of final product synthesized by COSHS from Reaction (1) with 4% PTFE

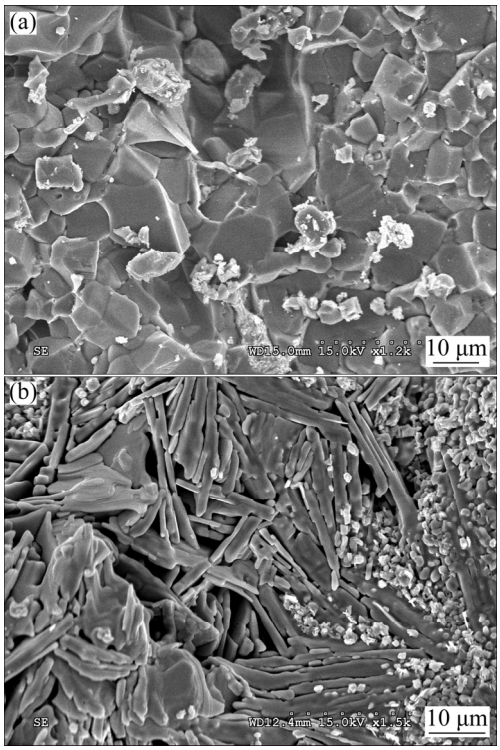

Fig. 7 SEM micrographs illustrating fracture surface of SHS-derived products synthesized: (a) Conventional SHS of Reaction (1) with 2% PTFE; (b) COSHS of Reaction (1) with 4% PTFE

respectively. Figure 7(a) is associated with the product of Reaction (1) with 2% PTFE and exhibits granular ZrC crystals with a size of about 10−20 μm and fine bright Al_2O_3 particles of 2−5 μm. A COSHS product is displayed in Fig. 7(b), showing that the ternary carbide $Zr_2Al_3C_4$ has a different morphology from ZrC. The columnar or plate-like grains in Fig. 7(b) are $Zr_2Al_3C_4$ and fine bright particles of 1−2 μm are Al_2O_3. $Zr_2Al_3C_4$ grains are about 2 μm in thickness and 10−30 μm in length, and some of them are closely stacked into a laminated configuration. The morphology of $Zr_2Al_3C_4$ grains shown in Fig. 7(b) is similar to that observed by GUO et al [11].

4 Conclusions

1) Formation of the $Zr_2Al_3C_4$−Al_2O_3 composite was investigated by PTFE- and chemical oven-activated combustion synthesis. The starting materials included ZrO_2, Al, and carbon black powders, and 2%−4% (mass fraction) PTFE that was employed as a reaction promoter and a carburizing agent. Experiments were conducted under the conventional SHS and COSHS configurations. By means of the conventional SHS scheme, self-sustaining combustion was characterized by a localized reaction zone propagating in a spinning mode. With the increase of the PTFE content from 2% to 4%, the combustion front velocity increased from 3.18 to 4.31 mm/s and combustion temperature from 1152 to 1272 °C. However, the as-synthesized product was a ZrC−Al_2O_3 composite with a trivial amount of $Zr_2Al_3C_4$. This was attributed to the low combustion temperature, insufficient reaction time, and evaporation loss of Al.

2) The COSHS method employed a composite sample consisting of a Ti/C booster shell and a core reactant compact. Combustion of the Ti/C mixture provided the core sample with a large amount of heat to raise its reaction temperature up to 1576 °C. In addition, the outer shell prolonged the dwell time at high temperatures for the core sample and prevented Al vapor from escaping away. Formation of $Zr_2Al_3C_4$ was greatly improved by COSHS and the as-synthesized product was a $Zr_2Al_3C_4$−Al_2O_3 composite with $Zr_3Al_3C_5$ as the minor phase. $Zr_2Al_3C_4$ grains had a plate-like morphology with a thickness of about 2 μm and length of 10−30 μm. Most of the long $Zr_2Al_3C_4$ laminas were tightly stacked and some were closely interlocked.

Acknowledgements

This research was sponsored by the Ministry of Science and Technology of Taiwan, China, under the grant of MOST 105-2221-E-035-039-MY2. Authors are grateful for the Precision Instrument Support Center of Feng Chia University in providing materials characterization facilities.

References

[1] BARSOUM M W. The $M_{N+1}AX_N$ phases: A new class of solids; thermodynamically stable nanolaminates [J]. Progress in Solid State Chemistry, 2000, 28: 201−281.

[2] EKLUND P, BECKERS M, JANSSON U, HÖGBERG H, HULTMAN L. The $M_{n+1}AX_n$ phases: Materials science and thin-film processing [J]. Thin Solid Films, 2010, 518: 1851−1878.

[3] WANG X H, ZHOU Y C. Layered machinable and electrically conductive Ti_2AlC and Ti_3AlC_2 ceramics: A review [J]. Journal of

Material Science and Technology, 2010, 26: 385−416.
[4] LIN Z J, ZHOU M J, HE L F, ZHOU Y C, LI M S, WANG J Y. Atomic-scale microstructures of $Zr_2Al_3C_4$ and $Zr_3Al_3Z_5$ ceramics [J]. Acta Materialia, 2006, 54: 3843−3851.
[5] HE L F, ZHONG H B, XU J J, LI M S, BAO Y W, WANG J Y, ZHOU Y C. Ultrahigh-temperature oxidation of $Zr_2Al_3C_4$ via rapid induction heating [J]. Scripta Materialia, 2009, 60: 547−550.
[6] ZHANG J, HE L, ZHOU Y. Highly conductive and strengthened copper matrix composite reinforced by $Zr_2Al_3C_4$ particulates [J]. Scripta Materialia, 2009, 60: 976−979.
[7] SCHUSTER J C, NOWOTNY H. Investigation of the ternary systems (Zr, Hf, Nb, Ta)−Al−C and studies on complex carbides [J]. Zeitschrift fuer Metallkunde, 1980, 71: 341−346.
[8] FUKUDA K, MORI S, HASHIMOTO S. Crystal structure of $Zr_2Al_3C_4$ [J]. Journal of American Ceramics Society, 2005, 88(12): 3528−3530.
[9] HE L, LIN Z, WANG J, BAO Y, LI M, ZHOU Y. Synthesis and characterization of bulk $Zr_2Al_3C_4$ ceramic [J]. Journal of American Ceramics Society, 2007, 90(11): 3687−3689.
[10] LAI C C, TUCKER M D, LU J, JENSEN J, GRECZYNSKI G, EKLUND P, ROSEN J. Synthesis and characterization of $Zr_2Al_3C_4$ thin films [J]. Thin Solid Films, 2015, 595: 142−147.
[11] GUO Q, YANG Y, LI J, SHEN Q, ZHANG L. In situ synthesis and properties of $Zr_2Al_3C_4/ZrB_2$ composites [J]. Materials and Design, 2011, 32: 4289−4294.
[12] MERZHANOV A G. Combustion and explosion processes in physical chemistry and technology of inorganic materials [J]. Russian Chemical Reviews, 2003, 72: 289−310.
[13] HOU H, NING X, WANG, GAO B, LIU Y, LIU Y. Preparation of $Mo(Si,Al)_2$ feedstock used for air plasma spraying [J]. Transactions of Nonferrous Metals Society of China, 2016, 26: 2939−2946.
[14] YEH C L, SHEN Y G. Combustion synthesis of Ti_3AlC_2 from Ti/Al/C/TiC powder compacts [J]. Journal of Alloys and Compounds, 2008, 466: 308−313.
[15] YEH C L, SHEN Y G. Effects of TiC and Al_4C_3 addition on combustion synthesis of Ti_2AlC [J]. Journal of Alloys and Compounds, 2009, 470: 424−428.
[16] YEH C L, SHEN Y G. Effects of Al content on formation of Ta_2AlC by self-propagating high-temperature synthesis [J]. Journal of Alloys and Compounds, 2009, 482: 219−223.
[17] ZHU J F, YE L, HE L H. Effect of Al_2O_3 on the microstructure and mechanical properties of Ti_3AlC_2/Al_2O_3 in situ composites synthesized by reactive hot pressing [J]. Ceramics International, 2012, 38: 5475−5479.
[18] ZHU J, HAN N, WANG A. Synthesis, microstructure and mechanical properties of $(Ti_{1-x},Nb_x)_2AlC/Al_2O_3$ solid solution composites [J]. Materials Science and Engineering A, 2012, 538: 7−12.
[19] ZHU J, JIANG H, WANG F, YANG C, XIAO D. Synthesis, microstructure and mechanical properties of Cr_2AlC/Al_2O_3 in situ composites by reactive hot pressing [J]. Journal of European Ceramics Society, 2014, 34: 4137−4144.
[20] YEH C L, KUO C W, CHU Y C. Formation of Ti_3AlC_2/Al_2O_3 and Ti_2AlC/Al_2O_3 composites by combustion synthesis in Ti−Al−C−TiO_2 systems [J]. Journal of Alloys and Compounds, 2010, 494: 132−136.
[21] YEH C L, KUO C W. An investigation on formation of Nb_2AlC by combustion synthesis of Nb_2O_5−Al−Al_4C_3 powder compacts [J]. Journal of Alloys and Compounds, 2010, 496: 566−571.
[22] SONG X, CUI H, CAO L, GULYAEV P Y. Microstructure and evolution of $(TiB_2+Al_2O_3)$/NiAl composites prepared by self-propagation high-temperature synthesis [J]. Transactions of Nonferrous Metals Society of China, 2016, 26: 1878−1884.
[23] XU J, ZHANG B, JIANG G, LI W, ZHUANG H. Synthesis of $SiC_w/MoSi_2$ powder by the chemical oven self-propagating combustion method [J]. Ceramics International, 2006, 32: 633−636.
[24] ESPARZA A A, SHAFIROVICH E. Mechanically activated combustion synthesis of molybdenum borosilicides for ultrahigh-temperature structural applications [J]. Journal of Alloys and Compounds, 2016, 670: 297−305.
[25] LEE T H, NERSISYAN H H, JEONG H G, LEE K H, NOH J S, LEE J H. Efficient synthesis route to quasi-aligned and high-aspect-ratio aluminum nitride micro- and nanostructures [J]. Chemical Engineering Journal, 2011, 174: 461−466.
[26] ZURNACHYAN A R, KHARATYAN S L, KHACHATRYAN H L, KIRAKOSYAN A G H. Self-propagating high temperature synthesis of SiC−Cu and SiC−Al cermets: Role of chemical activation [J]. International Journal of Refractory Metals and Hard Materials, 2011, 29: 250−255.
[27] MUSA C, LICHERI R, MONTINARO S, ORRÙ R, CAO G. Tantalum carbide products from chemically-activated combustion synthesis reactions [J]. Ceramics International, 2017, 43: 12844−12850.
[28] YEH C L, LIN J Z. Combustion synthesis of Cr−Al and Cr−Si intermetallics with Al_2O_3 additions from Cr_2O_3−Al and Cr_2O_3−Al−Si reaction systems [J]. Intermetallics, 2013, 33: 126−133.
[29] MUNIR Z A, ANSELMI-TAMBURINI U. Self-propagating exothermic reactions: The synthesis of high-temperature materials by combustion [J]. Materials Science Reports, 1989, 3: 277−365.
[30] BINNEWIES M, MILKE E. Thermochemical Data of Elements and Compounds [M]. Weinheim, New York: Wiley-VCH Verlag GmbH, 2002.

结合 PTFE 与热激化的燃烧合成原位生成 $Zr_2Al_3C_4/Al_2O_3$ 复材

Chun-liang YEH, Yi-Chang CHEN

Department of Aerospace and Systems Engineering,
Feng Chia University, 100 Wenhwa Road, Seatwen, Taichung 40724, Taiwan, China

摘　要：采用自蔓延燃烧合成(SHS)结合 ZrO_2 铝热还原与 PTFE 化学激化制备 $Zr_2Al_3C_4$–Al_2O_3 复材。原料包括氧化锆、铝、碳黑和 PTFE 粉末。除了传统的 SHS 方法外，合成实验以化学炉辅助的燃烧合成法(COSHS)进行。实验发现，达成自蔓延燃烧的最低 PTFE 含量为 2%(质量分数)。当使用传统 SHS 方法时，由于燃烧温度低(1152~1272 °C)且反应时间不足，合成复材中主要的碳化物为 ZrC，而不是 $Zr_2Al_3C_4$。但是，当应用 COSHS 技术时，燃烧温度可提高至 1576 °C，而且反应在高温下的时间增长，同时可避免铝蒸气的流失；因此，可以成功制备内含少许 $Zr_3Al_3C_5$ 的 $Zr_2Al_3C_4$−Al_2O_3 复材。$Zr_2Al_3C_4$ 晶粒为平板状，厚度约 2 μm，长度约 10~30 μm，多数晶粒紧密堆栈成层状微结构。

关键词：$Zr_2Al_3C_4$；燃烧合成；PTFE 激化；化学炉燃烧合成；铝热还原

(Edited by Bing YANG)